Medical Engineering & Physics 34 (2012) 665–680

Contents lists available at SciVerse ScienceDirect

Medical Engineering & Physics

journal homepage: www.elsevier.com/locate/medengphy

Needle–tissue interaction forces – A survey of experimental data

Dennis J. van Gerwen*, Jenny Dankelman, John J. van den Dobbelsteen

Delft University of Technology, Department of Biomechanical Engineering, Mekelweg 2, 2628 CD, Delft, The Netherlands

ARTICLE INFO

Article history:
Received 6 June 2011
Received in revised form 31 January 2012
Accepted 22 April 2012

Keywords:
Puncture
Friction
Cutting
Resistance
Insertion

ABSTRACT

The development of needles, needle–insertion simulators, and needle-wielding robots for use in a clinical environment depends on a thorough understanding of the mechanics of needle–tissue interaction. It stands to reason that the forces arising from this interaction are influenced by numerous factors, such as needle type, insertion speed, and tissue characteristics. However, exactly *how* these factors influence the force is not clear. For this reason, the influence of various factors on needle insertion-force was investigated by searching literature for experimental data. This resulted in a comprehensive overview of experimental insertion-force data available in the literature, grouped by factor for quick reference. In total, 99 papers presenting such force data were found, with typical peak forces in the order of 1–10 N. The data suggest, for example, that higher velocity tends to decrease puncture force and increase friction. Furthermore, increased needle diameter was found to increase peak forces, and conical needles were found to create higher peak forces than beveled needles. However, many questions remain open for investigation, especially those concerning the influence of tissue characteristics.

Contents

* Corresponding author.
E-mail address: d.j.vangerwen@tudelft.nl (D.J. van Gerwen).

1350-4533/$ – see front matter © 2012 IPEM. Published by Elsevier Ltd. All rights reserved.
http://dx.doi.org/10.1016/j.medengphy.2012.04.007

1. Introduction

Needles are common medical tools, yet considerable skill is required to use them effectively and safely. Developments in the fields of medical simulation and robotics, aimed at improving needle intervention efficacy, require a thorough understanding of needle–tissue interaction mechanics.

1.1. Background

The development of theoretical models that describe the interaction between needle and tissue, in terms of loads and displacements, has received a lot of attention in recent years (e.g. [1–3]). These models form an essential component of virtual-reality simulators with force feedback, intended for skills training. Moreover, they are indispensable for the development of new types of needles and needle-insertion robots.

Validation of these theoretical models is essential, especially for medical applications, and this requires reliable experimental data. However, for both practical and ethical reasons, experimental data from needle insertions into living biological tissue are rather difficult to come by.

To provide a starting point for researchers in this field, we have performed a survey of the experimental data available in the literature.

1.2. Related work

Other researchers have reviewed the theory behind mathematical models for needle–tissue interaction, but none of them focused explicitly on experimental data.

Abolhassani et al. [1] provide an overview of research related to needle insertion into soft-tissue with a broad scope, covering topics such as needle modeling, tissue modeling, and the application of these models to automated needle insertion.

Misra et al. [2] present an extensive review of literature related to the modeling of tool–tissue interaction for use in virtual-reality simulation. Topics covered include continuum mechanics and finite element methods, and their application to modeling of non-invasive as well as invasive tool–tissue interaction. Experimental methods for parameter identification and validation are also discussed briefly.

Cowan et al. [3] provide a thorough discussion of needle–tissue interaction models, path planning methods and imaging options in relation to robotic needle steering, but experimental findings receive little attention.

The survey of force sensing techniques presented by Trejos et al. [4], although mainly aimed at general minimally invasive surgery, helps to clarify the difficulties encountered when measuring instrument–tissue interaction forces in a clinical setting.

The current work is different from these reviews because it focuses solely on collecting and interpreting experimental data available in literature.

1.3. Aim

The mechanical interaction between needle and biological tissue is influenced by a great number of variables, e.g. related to insertion method, needle characteristics, and tissue characteristics. The aim of this survey is to collect experimental data that show *how* the axial needle force is influenced by these variables, and to guide the reader to the relevant literature. In addition, quantitative force information is collected and areas open for further research are identified.

1.4. Survey method

The survey is limited to those papers that present original force measurement data obtained during insertion of a needle (or similar tool) into any kind of soft material, either artificial or biological, living or dead.

The search was conducted during the last months of 2010, using the PubMed database (medical literature), the Scitopia.org search engine (technical literature), and Google Scholar.[1]

[1] A typical search string is: *(needle* OR cannula) AND (force* OR haptic* OR resistance OR friction) AND (measur* OR instrument*) AND (insert* OR advanc* OR displace* OR position* OR introduc* OR punctur* OR interact*)*

Table 1
Classification of papers by information content, indicating usefulness for the current survey.

Class	Criteria	References
C3	Methods clear, data presented with variability and sample size, and some form of statistical analysis	[5–16]
C2	As C3, but no statistical analysis	[17–30]
C1	As C2, but data are presented without indication of variability or sample size	[31–73]
C0	As C1, but description of methods not clear or incomplete (e.g. needle diameter not mentioned)	[74–103]

Table 2
Maximum axial force values found in all papers.

Description	*n*	Median [N]	Min–Max [N]
Total axial force	63	5.0	0.00004 [49] to 92.0 [18]
Puncture force	24	1.22	0.0005 [101] to 19.2 [63]
Cutting force	10	0.95	0.05 [30] to 1.3 [9]
Friction force	10	1.0	0.15 [24] to 2.8 [59]

Relevant papers were selected by considering title and abstract, and subsequently by examining tables and figures for useful information. In addition, references found in these papers were investigated. This resulted in a total of 99 papers.

Details of experimental methods and results were extracted manually and stored in a custom database. Using this database, the papers were objectively classified into four categories as shown in Table 1 (based purely on information content). A paper with C3 classification is more likely to be useful for the current survey than one with classification C0. However, it is stressed here that this classification is not a measure of quality: a C0 paper can still be of high quality.

The survey is structured in such a way that relevant literature is discussed by topic. The intention is to allow the reader to quickly skip to the topic of interest without having to read the entire survey.

2. Axial force characteristics

A typical medical needle consists of a slender stainless steel tube or 'cannula', with a plastic hub on one end and a sharp tip on the other. The hollow space inside the cannula is called the lumen. The tip is the part of the cannula that has varying cross-section, whereas the shaft has constant cross-section.

Axial force is defined here as the force acting on the needle hub in the direction of insertion. As will be discussed in the following sections, the axial force can consist of puncture force, cutting force, and friction force.

2.1. Magnitude of axial forces

The order-of-magnitude of needle–tissue interaction forces represents an important practical consideration for many applications. However, due to the large number of variables involved in needle tissue interaction, and the large variety of experimental approaches, it is difficult to give a comprehensive overview of all the forces encountered.

To provide at least some indication of the order-of-magnitude of forces typically encountered, the medians and extrema of the maximum axial forces found in all papers (irrespective of experimental conditions, etc.) are presented in Table 2. The large range of forces is mainly due to atypical needle diameters (30μm [49] to 11 mm [18]). The median is used because it is insensitive to these extrema.

2.2. Needle insertion phases

During needle insertion into soft-tissue, the motion of the needle relative to the surrounding tissue needs to be considered, rather than the absolute motion of the needle. By looking at the position of a needle relative to a tissue boundary, it is possible to distinguish three basic phases of interaction, as depicted in Fig. 1. These phases may be repeated when the needle encounters internal structures or variations in tissue properties. Similar penetration phases are described in the German industry standard for hypodermic needle tips, DIN 13097.

2.2.1. Phase 1: Boundary displacement

The first phase (Fig. 1b) starts when the needle comes into contact with the tissue boundary, and ends when the tissue boundary is breached. The actual breaching of the boundary is referred to as the puncture event.

During the boundary displacement phase, the tissue boundary deflects under the influence of the load applied by the needle tip, but the needle tip does not penetrate the tissue (the boundary moves along with the needle). This phenomenon is known as "tenting" [51,54].

A typical force–time curve is shown in Fig. 2. This figure was borrowed from Kobayashi et al. [21], who specifically measured the tissue displacement and investigated relative velocity during insertion.

This figure clearly shows a non-linear increase in force during the boundary displacement phase (relative velocity is zero). The shape of this curve is reminiscent of the load increase during thin-membrane displacement as found by e.g. Selvadurai [104]. Similar non-linear behavior of the axial force during boundary displacement is found in nearly all studies included in this survey.

At some point, the relative velocity starts to increase, which indicates that puncture has occurred. The puncture event and the processes at work during the post-puncture phases (phases 2 and 3) can be described using fracture mechanics theory, as shown by Mahvash and Dupont [55], Nguyen [63], Shergold and Fleck [71], Azar and Hayward [37], and Mahvash and Hayward [105].

As the needle displaces the tissue boundary, the load at the needlepoint increases, as do the stresses in the tissue surrounding the contact area. Once these stresses exceed a certain critical value, according to Kobayashi et al. [7], a crack will be initiated in the tissue and the needle will start to penetrate the tissue.

The work of Shergold and Fleck [71] and that of Azar and Hayward [37] suggests that the shape of this crack depends on the shape of the needle tip. A planar crack is initiated when using sharp bevel needles or conical needles. Diamond tips were found to create star shaped cracks, and needles with a very large bevel angle were found to create ring cracks, as illustrated by Fig. 3. This result was found for artificial gels as well as for porcine skin and porcine liver ex vivo, and for human skin in vivo. Once a crack has been initiated, phase 2 commences.

2.2.2. Phase 2: Tip insertion

The second phase (Fig. 1c) starts when the tissue boundary is breached, and ends when the tissue-boundary slides from the tip onto the shaft. During this phase, as the needle is advanced, the crack in the tissue-boundary is enlarged. The cut made by the sharp edges of the tip is wedged open by the increasing cross-sectional area of the tip, as described by e.g. Mueller [24].

The crack growth process can be either gradual, stable crack growth (cutting), or sudden, unstable crack growth (rupture), depending on the local properties of the tissue, such as rupture

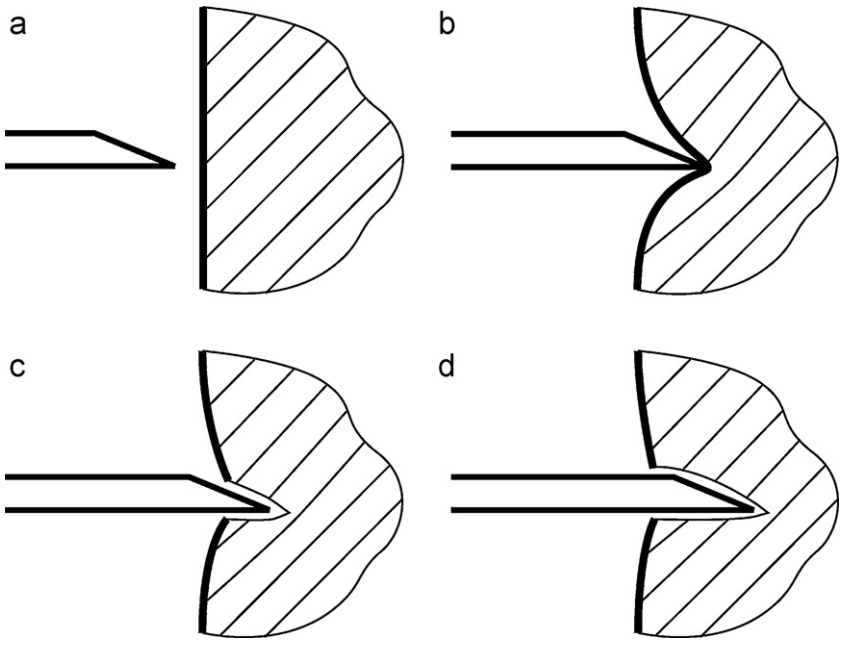

Fig. 1. Basic phases in needle insertion: (a) no interaction; (b) boundary displacement; (c) tip insertion; (d) tip and shaft insertion.

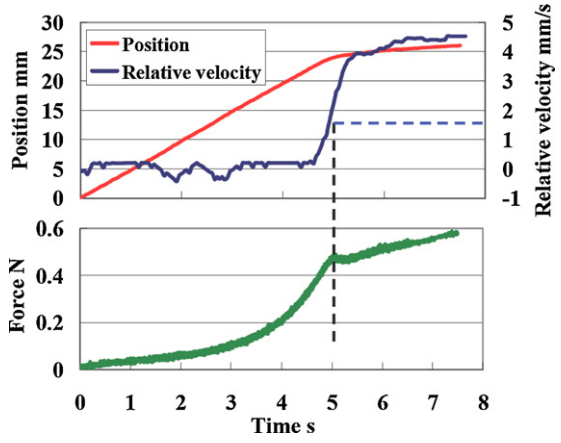

Fig. 2. Distinction between the pre-puncture and post-puncture phases based on relative velocity, for a 17 G beveled needle inserted into porcine liver ex vivo, at 5 mm/s [21]. Position is that of the tissue boundary.

toughness (i.e. the work required to cut the tissue, per unit cross-section area), and on the amount of strain energy stored in the tissue due to deformation.

When a thin membrane is punctured, the amount of energy stored during the boundary displacement phase is often so large that rupture occurs (sudden crack extension). This results in a (relatively large) drop in force, as the accumulated strain energy is used to extend the crack (an irreversible process). Rupture continues until the strain energy levels become low enough for the crack extension to proceed in a stable manner (i.e. cutting).

A needle traversing an internal tissue boundary can cause rupture when the toughness of the new tissue layer is significantly lower than that of the current tissue layer, according to Mahvash and Dupont [55].

The transition from tip to shaft may also give rise to an increase in axial force, due to the hole in the tissue boundary being wedged open. The magnitude of this effect depends on needle type, as will be discussed later.

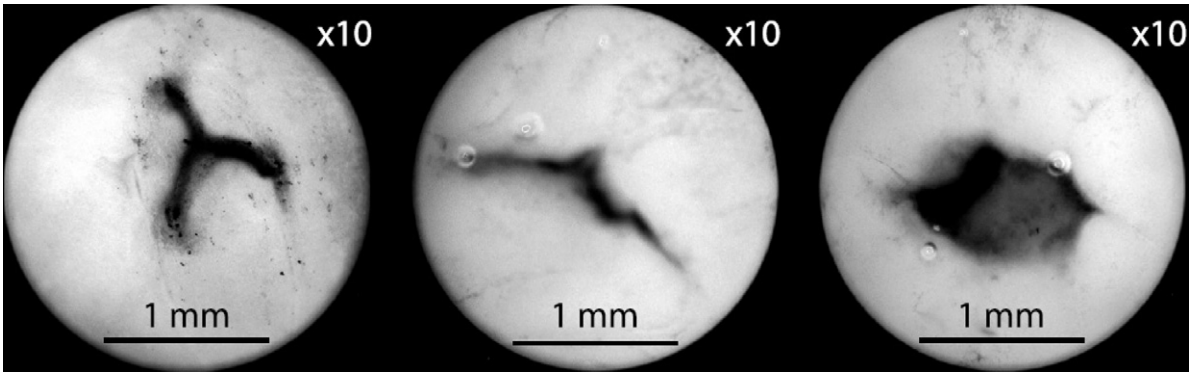

Fig. 3. Crack shapes in fresh porcine liver. Left-to-right: triangular diamond tip, small bevel angle, very large bevel angle. (With kind permission from Springer Science + Business Media: [37] Fig. 3).

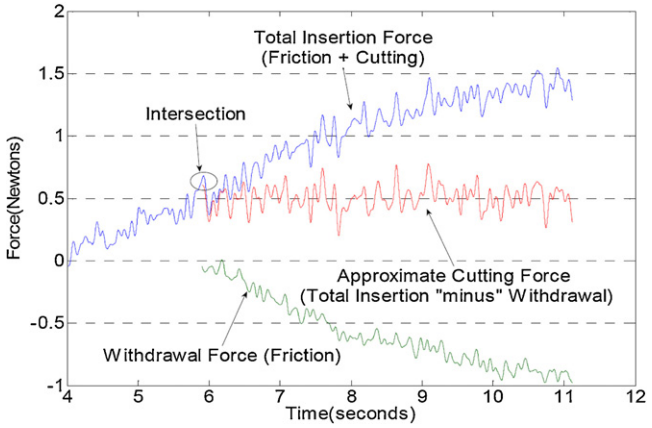

Fig. 4. Cutting force estimation by subtracting withdrawal force from insertion force [19]. (18 G diamond tip needle at 13 mm/s in porcine liver ex vivo.)

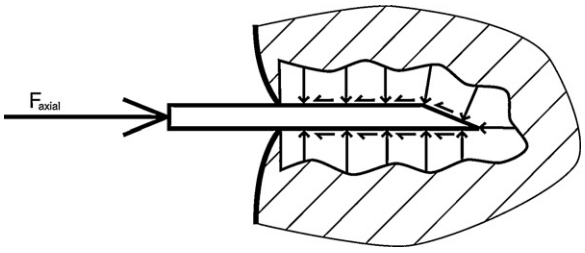

Fig. 5. Axial force acting on the base of the needle and surface forces acting on the tip and on the part of the cannula inside the tissue. Forces and moments will typically act on the hub in all directions, but focus here is only on the axial force since this is considered the most important.

2.2.3. Phase 3: Tip and shaft insertion

The third phase (Fig. 1d) starts just after the transition from tip to shaft and ends when the needle is stopped or when a new (internal) tissue boundary is encountered. During this phase, the contact area between tip and tissue and the size of the hole at the boundary remain more or less constant. Only the contact area between shaft and tissue increases as the needle is advanced.

During this phase the needle is subject to cutting (or rupture) forces at the tip, and to a varying friction force that is due to the increasing contact area between shaft and tissue.

Hing et al. [19], found that the stable cutting force is more or less constant, in porcine liver ex vivo, with some fluctuations due to rupture (small internal puncture events), depending on the level of inhomogeneity of the tissue. These findings were based on 45 insertions of diamond tip needles at 13 mm/s. Results for a single insertion are depicted in Fig. 4.

Their approach was based on the assumption that the axial force is composed of a cutting force and a friction force. Evidence in support of this assumption is discussed next.

2.3. Components of the axial force

Interaction between needle and tissue results in distributed loads along the needle–tissue interface, that is, along the contact area between needle and tissue, as depicted in Fig. 5. These surface forces consist of normal and tangential tractions acting on the contact surface, as mentioned by e.g. [58,96]. An important question is how these loads are distributed along the needle.

Since direct measurement of such a load distribution is practically impossible, indirect methods need to be used. This implies that one has to resort to the use of needle–tissue interaction models to reconstruct the load distribution along the needle based on external force measurements and tissue displacement measurements.

Artificial materials are generally easier to model than biological tissues, since the latter are composite structures and thus are inhomogeneous and anisotropic.

2.3.1. Load distribution in artificial materials

DiMaio and Salcudean [41,82,42] employed finite element (FE) models to extract an approximate axial load distribution based on axial force measurements and tissue-displacement measurements in PVC phantoms. The load distribution along the needle was found to be largely uniform, with the exception of a peak near the tip, as depicted in Fig. 6. Although no explanation is given for this peak, it is reasonable to assume that it is related to the mechanical processes at work near the tip (cutting/rupture). The large uniform part of the distribution is supposedly due to friction.

Dehghan et al. [79] used a three-parameter model (shaft height, peak height, peak width) to approximate that same distribution (Fig. 6), and identified these parameters using a finite element approach similar to that of DiMaio and Salcudean [42]. The peak widths found for insertions into artificial phantom material are in the same order of magnitude as the needle tip length, which supports the assumption that the peak is due to the cutting process.

Crouch et al. [17], used a similar approach, based on a FE model and measurements of tissue displacement and force, to estimate the load distribution along an 18 G diamond tip needle in a silicone gel. Their approach focused on the influence of needle velocity. The distribution shape was approximated using cubic splines and also shows a large uniform part together with a peak at the tip. A drop in force is observed, just behind the peak, but no explanation is given for this peculiarity.

The detailed distribution of loads along the tip of a beveled needle is investigated by Misra et al. [96], but they only consider transverse forces.

Note that a constant force density (force per unit length) along the cannula, i.e. a uniform load distribution, corresponds to a linear force-position relation with slope equal to the force density. This knowledge is useful when considering biological tissue.

2.3.2. Load distribution in biological tissue

In the aforementioned, the axial load distribution was found to be largely uniform when the needle is inserted into homogeneous isotropic artificial materials. The question now is whether this is also true for biological tissue.

The FE approach is not practical here, due to difficulties in modeling biological tissue and in measuring internal tissue displacement. However, if the load distribution does indeed remain uniform, this would result in a linear rise of friction force with insertion distance, or in a constant friction force if the contact area remains constant during insertion. In order to verify this, friction force needs to be measured somehow.

Different approaches can be adopted for measuring the friction force acting on a needle. For example, Hing et al. [19,20] assume that the force during removal of the needle is due to friction only, thereby yielding a direct friction measurement. The resulting friction curve shown in Fig. 4, for porcine liver, can be interpreted as approximately linear.

Another approach is to make sure that the needle tip is outside the tissue on the other side, thereby ensuring that the tip no longer interacts with the tissue and the force measured is only due to friction along the cannula. This method, in combination with unidirectional motion, is used by Abolhassani et al. [31] (turkey muscle), and Kobayashi et al. [21] (porcine liver), resulting in approximately constant friction force (as the contact area between needle and tissue remains constant).

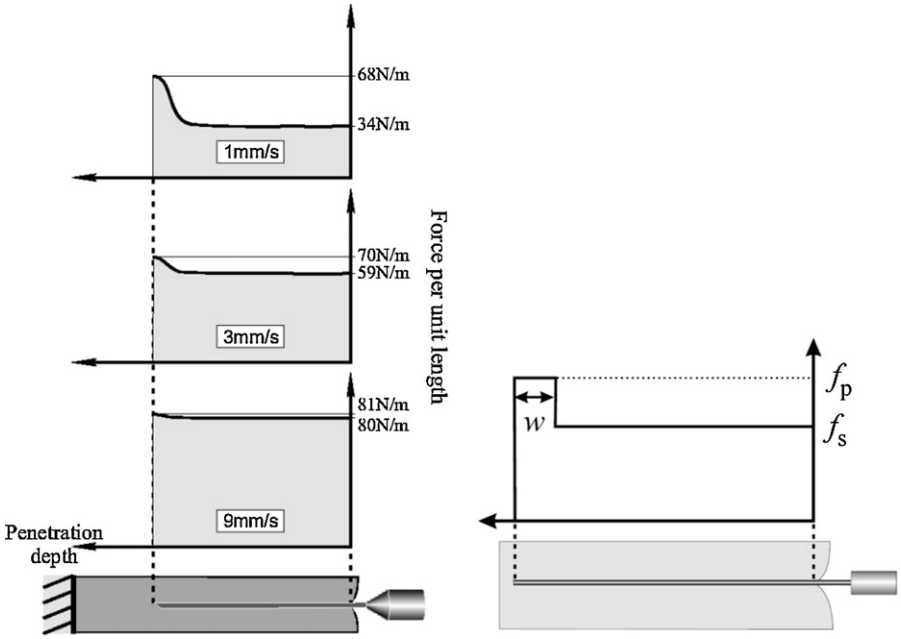

Fig. 6. Distribution of axial load along a 17 G Tuohy needle at different velocities in a PVC phantom [42] (© 2003 IEEE), and the three-parameter model used by Dehghan et al. [79] to approximate this distribution, with peak width w, peak force density f_p and shaft force density f_s.
(With kind permission from Springer Science+Business Media: [79] Fig. 3b.)

The same approach is used by Simone and Okamura [72,73], O'Leary et al. [64], and Okamura et al. [9] (bovine liver). Using bi-directional motion, they investigated of static as well as dynamic components of friction force.

Yet another approach is to measure the tip force and total force independently, as was done by Kataoka et al. [47] for a 17 G diamond tip needle in canine prostate ex vivo. Their special measurement device allowed indirect determination of the friction component based on the assumption that total insertion force is the sum of tip force and friction force. Their results seem to indicate that, during the post-puncture insertion phases, friction force does indeed increase linearly with insertion distance. However, in their findings the (friction) force does not change sign during retraction, which undermines the credibility of the results.

The above findings suggest that axial load distribution along the needle is approximately uniform, not only for (homogeneous, isotropic) artificial materials, but also for the biological tissues investigated here.

In addition, force vs. position diagrams presented by other authors, who did not explicitly measure friction, in many cases show an approximately linear rise in total force during the post-puncture phases. This too is consistent with the assumption that the total insertion force is composed of a constant force due to (quasi-steady) cutting and a linearly increasing force due to friction. Examples are provided by Meltsner et al. [57], Okamura et al. [9], O'Leary et al. [64], Podder et al. [65] for artificial materials, and by Healey et al. [43], Mahvash and Dupont [55], Kobayashi et al. [21] for biological tissue. Note that there are always some excursions due to e.g. internal puncture events, as found e.g. by Mahvash and Dupont [8] for porcine liver.

Note that Howard et al. [46], Jensen et al. [6] and Naemura [60] attempted to measure friction by inserting the needle twice at precisely the same location, under the assumption that all the cutting was done on the first insertion so that the force during the second insertion would be entirely due to friction. This approach is questionable because there is no reason to assume that the needletip will follow the exact same path without so much as scraping the tissue wall.

In short, three phases can be distinguished during basic needle insertion, based on the position of the tip relative to the tissue boundary. During insertion, crack initiation and stable or unstable crack extension processes occur, which are referred to as puncture, cutting, and rupture respectively. There are indications that cutting results in approximately constant force, and that the friction force increases approximately linearly with insertion depth in various materials. The following section investigates how the axial force components are influenced by insertion method.

3. Influence of insertion method

The interaction between needle and tissue is influenced by the way the needle is inserted. For example, manual insertion will yield different results than automated insertion. Likewise, force may be influenced by insertion velocity, axial rotation during insertion, location and direction of insertion, and by bevel orientation during insertion.

3.1. Manual vs. automated insertion

During clinical procedures, the clinician, needle and patient are all part of a complex dynamical system with many interactions. This means that there are many potential confounding factors.

To illustrate this point, an example of a force vs. position diagram for manual needle insertion during a clinical procedure and the corresponding velocity vs. position diagram are depicted in Fig. 7 [66].

Obviously, the velocity varies tremendously throughout the procedure, but it is not known whether this is deliberate, or if it is a result of the interaction between needle and tissue, or perhaps both. This makes interpretation of the forces difficult.

If a haptic simulator were developed for this procedure, the interaction between trainee and simulator would have to result in force and velocity characteristics like those presented in Fig. 7. On the other hand, for the systematic investigation of needle–tissue interaction, experiments at constant velocity would be preferable.

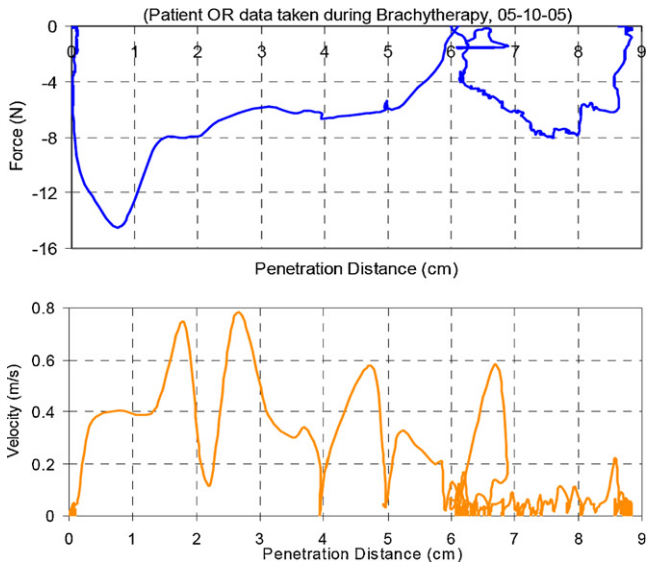

Fig. 7. Force and velocity vs. penetration distance measured during a clinical brachytherapy procedure [66] (© 2005 IEEE). The needle seems to be inserted in short bursts.

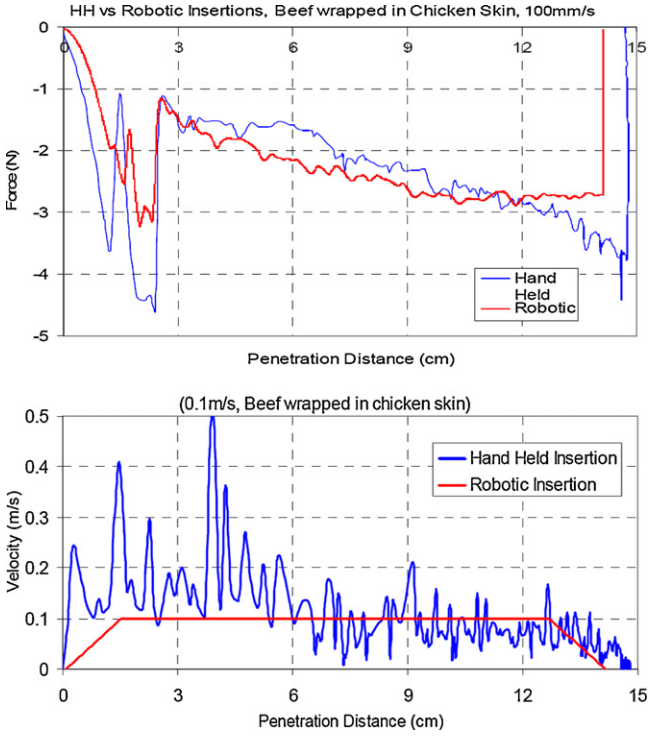

Fig. 8. The result of trying to maintain a constant velocity during manual (hand held) insertion and during robotic insertion into beef wrapped in chicken skin (average of five insertions at different locations) as presented by Podder et al. [66].
© 2005 IEEE.

A comparison between robotic insertion and manual insertion, both attempting to maintain the same constant velocity, is found in Fig. 8 [66]. The inability of the human to maintain a desired constant velocity during manual insertion is evident from this figure. This emphasizes the necessity of using robotic insertion devices to ensure controlled experimental circumstances.

3.2. Insertion velocity

The velocities encountered during actual clinical procedures may be relevant when investigating the influence of insertion velocity on axial force.

3.2.1. Insertion velocity during clinical procedures

A limited amount of information was found concerning typical velocities during clinical procedures.

Healey et al. [43] mention a speed of 500 mm/min (8.3 mm/s) as an approximation of the speed of needle insertion during interventional radiology procedures, but no source is provided. Hiemenz et al. [86] mention a video observation study of 20 epidural procedures which showed the insertion speed to range from 0.4 mm/s to 10 mm/s.

Abolhassani et al. [33] consider the range from 1 mm/s to 20 mm/s to be representative for prostate brachytherapy, based on feedback of physicians. Podder et al. [66,11,26] measured the velocity during more than 25 actual prostate brachytherapy procedures and found *peak* velocities in the order of 1000 mm/s, which is two orders-of-magnitude larger. This may seem strange at first, but it is not uncommon in clinical practice to insert the needle in short bursts, and Fig. 7 [66] shows that mean velocity during the initial phase of the insertion was in the order of 100 mm/s, whereas during the final approach, mean velocity was reduced to the order of 1 mm/s.

Whether or not based on these data, the majority of experiments included in this survey were performed at constant velocities in the order of 1–10 mm/s. Note that nearly all authors consider absolute needle insertion velocity, instead of that relative to tissue motion. This is not surprising given the practical difficulties in measuring relative motion.

In light of the differences between artificial materials and biological tissue, it is to be expected that velocity effects differ between the two types of material.

3.2.2. Velocity effects in artificial phantom materials

Five papers specifically investigated velocity effects during needle insertion into artificial phantom materials and presented results accordingly [17,42,57,61,65]. The latter considered the range from 5 mm/s to 200 mm/s, whereas the others all used velocities in the range from 1 mm/s to 20 mm/s.

Crouch et al. [17] considered insertion of an 18 G diamond tip needle into silicone gel at velocities of 3–21 mm/s in steps of 3, with video based tissue deformation tracking. They found a logarithmic relation between insertion force (at a fixed depth) and insertion velocity and a similar relation for the slope of the force-position curve (both increase with speed).

DiMaio and Salcudean [42] show that insertion speed influences the load distribution along the shaft (shaft force density), as depicted in Fig. 6. For a 17 G Tuohy needle in PVC gel, not only does the total force (i.e. total area under the distribution curve) increase with speed, but the peak in the distribution becomes smaller and disappears altogether at 9 mm/s, resulting in a fully uniform distribution. Thus, although cutting forces increase slightly with speed, friction forces increase much faster with speed and become dominant at higher speeds. The relation between shaft force density and velocity resembles the relation found for the total force vs. velocity by Crouch et al. [17].

Meltsner et al. [57] investigated the effect of needle insertion velocity on insertion force for both rotating needles and non-rotating needles. Insertions of 17 G bevel needles and conical needles into porcine gelatin at 5–20 mm/s (non-rotating) showed an increased slope of the force vs. position curve. The same trend appears to hold for rotating needles up to 5 rpm, although overall slopes are lower here.

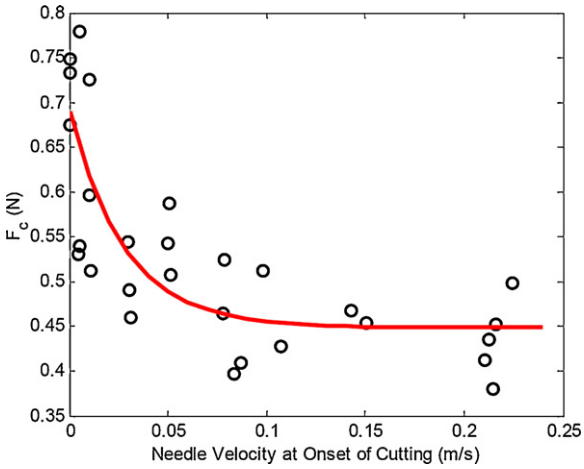

Fig. 9. Force required to initiate cutting (i.e. puncture force), as a function of insertion velocity, using a 19 G diamond tip needle in porcine heart tissue ex vivo ($n = 28$) as presented by Heverly and Dupont [44].

Podder et al. [65] investigated the effects of velocity on insertion force and tissue deflection, by inserting 18 G diamond tip needles into PVC gel under fluoroscopic imaging. Axial velocities of 5–200 mm/s were considered, also in combination with rotational velocities. The axial force vs. position curves for the non-rotating case clearly indicate an increase in slope with increasing velocity. This effect seems to persist if the needle is rotated (<5 Hz) during insertion.

Naemura et al. [61] investigated the effect of tip shape on the slope of the force-position curve just after puncture (force drop), during insertion of an 18 G Tuohy needle through silicone rubber membranes at 2–8 mm/s. No clear effect of velocity was observed.

In short, axial force in artificial materials, like PVC, silicone, or porcine gel, increases almost linearly with position. The slope of the force-position curve also increases (non-linearly) with velocity, suggesting an increase in friction.

3.2.3. *Velocity effects in biological tissue*

Eleven papers examine velocity effects during needle insertion into biological tissue [33,76,5,44,19,6,7,55,57,21,8]. Three of those, viz. [44,55,8], considered velocities larger than 25 mm/s (up to 250 mm/s).

Brett et al. [76] inserted Tuohy needles (unknown size) into porcine ligamentum flavum (2–5 h old) at 0.83–2.50 mm/s. Results indicate a decrease in puncture force with increasing velocity, but sample size is unknown. The puncture forces presented here are one order-of-magnitude higher than most of the other forces in this survey.

Heverly and Dupont [44] inserted a 19 G diamond tip needle into porcine heart (epicardium and myocardium), ex vivo, at velocities between 5 mm/s and 250 mm/s. In the epicardial layer they found a decrease in puncture force (force required to initiate cutting) with velocity up to 75 mm/s, and velocity independence at higher speeds, as depicted in Fig. 9. It is concluded that cutting force and tissue displacement can be minimized by maximizing velocity.

Mahvash and Dupont [55] conclude that both puncture force and tissue displacement at the moment of puncture decrease with increasing velocity. These conclusions are based on insertions of a 19 G diamond tip needle into porcine heart tissue, at speeds of 1–100 mm/s (five insertions per velocity). The difference in mean puncture force at 50 mm/s and 100 mm/s is very small compared to the standard deviation.

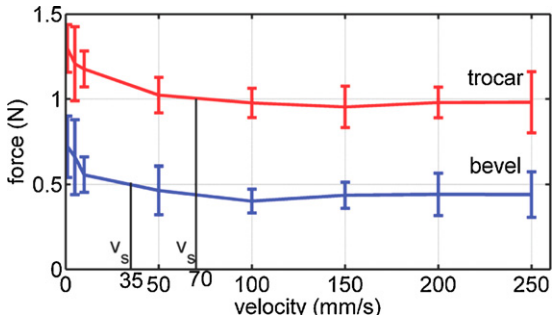

Fig. 10. Mean peak axial force, with standard deviation ($n = 10$), measured during insertion of 19 G diamond tip trocar needles and 18 G beveled needles into porcine heart [8].

Mahvash and Dupont [8] investigated the effect of insertion velocity on puncture force for 19 G diamond-tip trocar needles and 18 G beveled needles in porcine heart muscle, at speeds ranging from 1 mm/s to 250 mm/s. The results, based on 10 insertions per velocity, again show a decrease in puncture force with increasing velocity up to approximately 50 mm/s, as depicted in Fig. 10. At higher velocities the puncture force appears to remain constant. This trend holds for both needle types and is supported by statistical analysis.

Hing et al. [19,20] investigated the insertion of 18 G diamond tip needles into three different porcine liver samples, at 1.0–25.4 mm/s. Differences in mean cutting force and mean puncture force are small compared to their standard deviations, suggesting little or no effect of velocity. The variability in the puncture force does appear to decrease with increasing velocity.

Kobayashi et al. [7] performed needle insertions with a 17 G needle into porcine liver samples at 0.5–8 mm/s (9 insertions per velocity). Here again the median puncture force seems independent of velocity, whereas variability in puncture force seems to decrease with increasing velocity. On the other hand the median tissue displacement at the moment of puncture appears to decrease with velocity, whereas the variability in puncture displacement remains constant.

Kobayashi et al. [21] investigate the velocity dependence of frictional force, by inserting 17 G needles into 2cm thick sections of porcine liver at velocities ranging from 0.01 mm/s to 10 mm/s. Fig. 11 shows the result for initial frictional force as a function of velocity, based on a total of 60 insertions and 24 livers. The increase in friction force appears to be logarithmic for

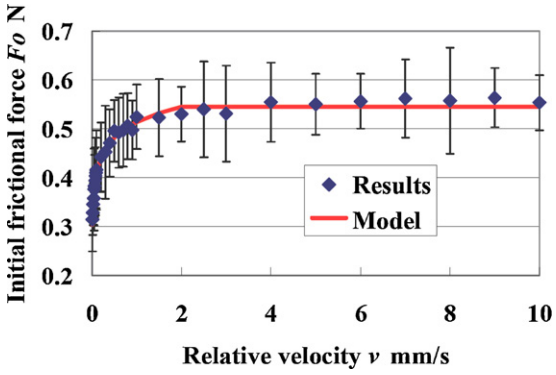

Fig. 11. Increase in frictional force for a 17 G needle in 2 cm thick porcine liver at constant speed [21] (24 livers, 60 insertions per measurement point, error bars undefined).

speeds up to 2 mm/s and remains constant for speed higher than that.

Abolhassani et al. [31–33] considered the insertion of an 18 G beveled needle into turkey breast (with skin) at 1–20 mm/s. Tissue displacement at the moment of puncture was found to decrease with increasing velocity.

Meltsner et al. [57] investigate the effect of needle insertion speed on total axial force for both rotating needles and non-rotating needles. Insertions of 17 G bevel needles and conical needles into bovine muscle at 5–20 mm/s show no clear trend.

Frick et al. [5] investigated the effect of velocity on insertion force for a straight (0.88 mm) suture needle, inserted into sheep skin at different skin-tension levels. Five insertions were performed for each combination of speed (1, 5, 10 mm/s) and skin-tension load (1, 3, 5 kg). This was repeated for three adjacent samples of skin, for a total of 135 insertions. No significant effect of velocity on axial force was found, although it is mentioned that statistical power is low. It should be noted here that this is the only study that considers statistical power or the number of insertions required to obtain sensible results.

In short, puncture force was found to decrease with increasing velocity in porcine heart, but remained constant at velocities over 50 mm/s. In porcine liver the mean puncture force seems independent of velocity, but its variability was found to decrease with increasing velocity. Friction force in porcine liver was found to increase with velocity up to 2 mm/s and remain constant at higher speeds. No effect of velocity on axial force was found in bovine muscle and sheep skin.

In addition to insertion velocity, axial needle rotation is also expected to influence the puncture force and the cutting force (due to drilling effects), as well as the friction force.

3.3. Axial rotation

Abolhassani et al. [31–34] inserted 18 G beveled needles into turkey tissue with skin, at a constant translational velocity of 10 mm/s with rotational frequencies ranging from 1 rpm to 25 rpm (0.02–0.42 Hz). Continuous rotation was considered, as well as rotational oscillation with amplitudes of 10°, 30°, and 90° for each frequency. Based on 20 insertions per condition (rotation type and frequency), both tissue displacement before puncture and friction force were found to be reduced by rotational motion. Reductions for both variables were in the order of 10% with respect to the non-rotating case. No clear influence of rotational frequency was found, but the range from 3 to 7 rpm (0.05–0.12 Hz) is suggested as optimal. Rotational oscillation is said to yield better results than continuous rotation, but it is not clear for which rotational speed.

Meltsner et al. [57] investigated the influence of needle rotation on needle placement accuracy and tissue damage. This was done by inserting 17 G beveled needles and 17 G conical needles into porcine gel and into beef phantoms, at insertion velocities of 5–20 mm/s and rotational frequencies of 0, 3, and 5 Hz (unidirectional rotation). In both materials, reductions in total axial force greater than 50% were achieved due to rotation of the (conical) needle.

Langevin et al. [51] investigate a phenomenon in acupuncture called needle grasp, referring to the sensation that the needle is grasped by the skin when pulled out. To this end, they measured pull-out force acting on 31 G acupuncture needles, after subjecting them to a specific rotation pattern (no-rotation, unidirectional, or bidirectional rotation) at a prescribed depth. Insertion velocity was 10 mm/s, rotational frequency 8 rpm (0.13 Hz), and pull-out velocity was 5 mm/s. Measurements were performed on 60 human test subjects, at 16 locations on the body. Needle rotation was found to cause a statistically significant increase in pull-out force in the order of 50% for bi-directional and 150% for unidirectional rotation (compared to no-rotation).

In short, axial rotation was found to reduce friction force in chicken breast, typically by 10%. It was found to reduce total axial force in porcine gel and in beef by up to 50%. In live human skin, rotation of acupuncture needles before pull-out was found to increase pull-out force by up to 150%.

3.4. Insertion location and direction

Biological tissue is typically inhomogeneous and anisotropic, i.e. the (mechanical) properties depend on position and orientation respectively. Therefore, it is important to consider the location at which the needle is inserted, as well as the direction of needle insertion with respect to the tissue.

A new location is selected for every insertion by Abolhassani et al. [33], Hing et al. [19], Hing et al. [20], Kataoka et al. [47], Lechner et al. [52], Mahvash and Dupont [55], Matsumiya et al. [22], Naemura et al. [61], Tran et al. [29], and Hiemenz Holton [45], but this was done to prevent the needle from following an existing path, not to investigate the influence of insertion location. Insertion location was randomized (within a specific area) by Westbrook et al. [15] and Mahvash and Dupont [8].

Three studies showed some form of systematic investigation of the influence of location on axial force:

Podder et al. [27] and Yan et al. [16] explicitly investigated differences in insertion forces between locations. This was done by inserting 18 G diamond tip needles into three different zones of human prostate ex vivo (including cancerous tissue). Axial forces in the different zones were comparable, but no clear conclusions were drawn in this respect.

Langevin et al. [51] found some statistically significant differences (post hoc) in pull-out force for acupuncture needles inserted into the skin of human subjects at different locations of the body, but no conclusion was drawn from this observation.

Crouch et al. [17], Healey et al. [43], Howard et al. [46], Langevin et al. [51], Matsumiya et al. [22], and Westbrook et al. [15] inserted their needles perpendicular to the tissue surface. Okuno et al. [25], Saito and Togawa [69], Saito and Togawa [28], and Hiemenz et al. [87] investigated needle insertions at other angles. However, none of the above explicitly investigated the influence of insertion angle on axial force.

Suzuki et al. [14] investigated the influence of insertion angle (30° and 45°) on axial force and hole shape during penetration of a polyethylene membrane by two catheter tips with different multi-faceted bevels ("Lancet" and "Backcut") at 3.3 mm/s (20 insertions per condition). Only for the "Backcut" type, axial force at 30° was found to be significantly lower (approx. 40%) than for 45°.

In short, information concerning the influences of insertion location or direction is scarce.

3.5. Bevel orientation

When a needle with a tip that is not cylindrically symmetrical, e.g. a beveled or diamond tip, is inserted into an anisotropic material, then it is important to consider the orientation of the bevel(s) with respect to the material (i.e. the angle of rotation about the longitudinal axis of the needle). Although this is recognized by Reed et al. [67], Abolhassani et al. [33], and Westbrook et al. [15], the only systematic investigation into the effects of bevel orientation was performed by Lewis et al. [54].

Lewis et al. [54] investigated the effect of bevel orientation on force required to puncture human dura (ex vivo) using a 17 G Tuohy needle. The needle was advanced at 20 mm/min (0.33 mm/s). The difference between puncture forces was investigated for bevel orientations parallel to and perpendicular to the dural fibers. The

needle oriented perpendicular to the dural fibers required approximately 30% higher force to penetrate the dura than the parallel one. This difference was found to be statistically significant ($p < 0.05$), based on a total of 40 insertions into 10 different dura specimens.

In short, bevel orientation with respect to tissue fibers appears to have a considerable influence on axial force in human dura.

In addition to insertion method, needle characteristics may also play an important role in needle–tissue interaction.

4. Influence of needle characteristics

Needles come in many shapes and sizes, and are primarily defined by tip type, diameter (expressed in wire gauge G), and length. The latter is not discussed here, although a longer needle could deflect more easily, which would influence the loads. Other factors that may influence the axial force are the presence of lubricants and the sharpness of the tip.

4.1. Diameter

The outer diameter of the cannula is specified according to the Stubs wire-gauge standard (ISO 9626), denoted by a capital G. Popular sizes range from 10 G (3.4 mm) to 30 G (0.31 mm), where a higher gauge indicates a smaller diameter.

Stellman [13] compared 18 G, 22 G, 26 G and 30 G beveled needles from different manufacturers, with different types of lubricant, by inserting them into polyurethane membranes at 1.7 mm/s. An increase in puncture force with diameter was observed, irrespective of lubrication type and manufacturer.

Shergold and Fleck [71] inserted conical tip needles (60° tip angle) with diameters 0.5 mm (25 G), 1 mm (19 G), and 2 mm (14 G) into silicone rubber at 0.8 mm/s. Peak axial force was found to increase with diameter.

Okamura et al. [9] and O'Leary et al. [64] investigated the influence of diameter on the average slope of the axial-force vs. position curve by inserting the needles into silicone rubber (three insertions per needle) at 2.65 mm/s (for 7 seconds). Two-way analysis of variance for three ranges of diameter (0.59–0.75 mm, 0.95–1.0 mm, and 1.55 mm) and three tip types (bevel, cone, diamond) showed statistically significant influence of diameter on force-position slope (slope increases with diameter). This is consistent with increased friction force. Significant interaction between factors was also found, suggesting that the effect of tip type is aggravated by increased diameter.

Okuno et al. [25] measured total axial force during puncture of human skin and vena mediana cubiti in ten human subjects, in vivo. Insertion was performed manually at approximately 15mm/s with 27 G and 21 G beveled needles. The results suggest an influence of needle diameter on peak axial force.

Podder et al. [11] measured total axial force during manual insertion of 18 G and 17 G diamond tip needles during clinical procedures on 20 patients (10 patients per needle size, with a total of 52 insertions). Results clearly suggest that peak axial force increases with needle diameter. In order to assess the influence of confounding factors, this conclusion was verified by inserting the needles into a PVC phantom under controlled circumstances. The effect was still present, albeit somewhat smaller. Similar results are found for 17 G and 18 G needles in 25 patients (72 insertions total) by Podder et al. [26,12].

In short, puncture force was found to increase with diameter for beveled needles in polyurethane. Peak axial force was found to increase with diameter in human tissue in vivo as well as in silicone rubber. The slope of the force-position curve in silicone was found to increase with diameter, which is consistent with an increase in friction. In addition, increased diameter was found to aggravate the effect of tip type in silicone.

4.2. Tip type

The function of the needle tip is to create a passage through tissue. This is typically achieved by a combination of cutting and wedging. The amount of force needed to cut a path, and the amount of tissue damage that arises as a result, depend on the shape of the needle tip. The most common needle tip shapes are depicted in Fig. 12.

4.2.1. Basic tip shape

Westbrook et al. [15] found that conical needles of various size lead to higher peak axial force than Quincke needles (i.e. multi-faceted bevel) when inserted manually into excised bovine dura, with bevel parallel to the fiber direction.

Shergold and Fleck [71] compared the peak axial force and crack propagation mechanisms for 1.0 mm (19 G) blunt and conical tip needles in two types of silicone rubber, at 0.8 mm/s. The conical needle showed a steady increase in peak axial force due to steady crack extension, the blunt needle exhibited much larger forces with unsteady crack extension.

Mahvash and Dupont [8] inserted 19 G diamond tip trocar needles and 18 G beveled needles into porcine heart ex vivo at a wide range of velocities. It was found that the diamond tip needle, despite its smaller diameter, consistently showed a peak axial force approximately twice as high as for the beveled needle. This is depicted in Fig. 10. It is not clear from the text whether this is due to the actual puncture or to the transition from stylet to shaft.

Okamura et al. [9] and O'Leary et al. [64] inserted conical, beveled, and diamond tip needles into silicone rubber at 2.65 mm/s. It was found that an increasing number of cutting edges (conical → beveled → diamond) leads to a decrease in slope of the axial-force vs. position curve (which is consistent with a decrease in friction force). This effect was shown to be statistically significant, and was shown to become stronger for larger diameters.

Meltsner et al. [57] inserted 17 G conical needles and beveled needles into porcine gelatin at 5, 10, and 20 mm/s. Differences in axial force were minimal. Photographs of the effect of tip type on gel damage are shown.

In short, conical tips produce higher peak axial force than Quincke bevels in bovine dura. Peak axial force for blunt tipped needles was much higher than for conical tips in silicone. Diamond tip trocar needles caused much higher peak axial force than beveled needles in porcine heart, despite smaller diameter. Furthermore, an increased number of cutting edges was found to decrease friction force in silicone.

4.2.2. Tip shape details

Details in the shape of the tip often lead to characteristic traits in the axial force.

Hing et al. [19,20] inserted a diamond tip trocar needle into porcine liver at velocities up to 25.4 mm/s. This kind of needle consists of a blunt cannula with a diamond tip stylet that protrudes fully from the cannula. It is observed that there are two peaks in the force-position curve: a small one due to the diamond tip (puncture) and a large one due to the transition from tip to shaft.

Stellman [13] discusses the detailed characteristics of the force-displacement curve during penetration of a polyurethane film using a 22 G beveled needle. A small peak was typically found for initial puncture of the membrane, followed by a large peak associated with the transition from bevel to shaft. This is illustrated by Fig. 13.

Sources from industry show similar results. Mueller [24] measured the axial forces for 18 G, 20 G, and 21 G multi-faceted bevel needles during 24 insertions into 0.4*mm* polyurethane membranes

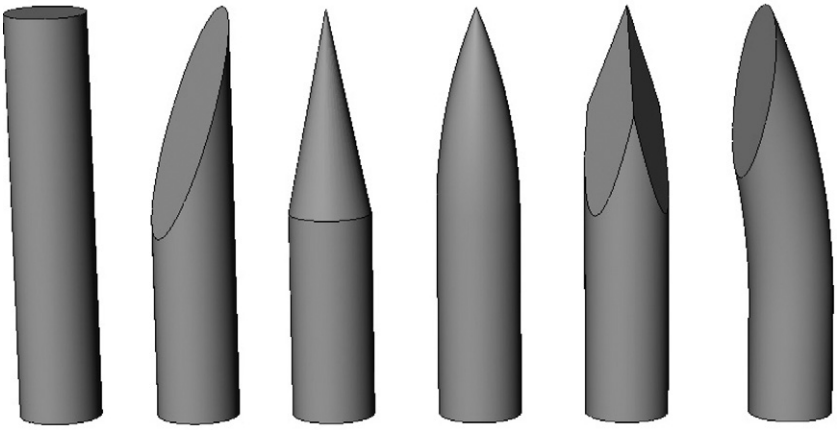

Fig. 12. Basic needle tip shapes (left-to-right): blunt, beveled, conical, Sprotte, diamond (Franseen), Tuohy. Note that there are many variations of the basic beveled tip, characterized by the presence of multiple facets (e.g. Quincke).

at 100*mm*/*min* (i.e. 1.67 mm/s). Distinct force peaks were observed at the moment of initial puncture, at the transition between facets, and at the transition from bevel to shaft. Mayer et al. [23] found the same kind of result for 27 G, 29 G and 30 G beveled needles. Both sources closely follow the methods described in the German industry standard DIN 13097 for hypodermic needle tips.

Nguyen et al. [63] present a force–displacement curve for a 25 G multi-faceted bevel needle inserted into a 0.8*mm* thick neoprene membrane at a very low speed of 0.05 mm/min (0.0008 mm/s). It shows that, under these circumstances, crack initiation (i.e. puncture) occurs well before the peak force is reached. The peak force is found to occur at the moment the tip protrudes at the other side of the membrane.

Naemura [60] investigates differences in tip shape between six 18 G Tuohy needles from different manufacturers, but no useful conclusions are drawn. Tuohy needles have a bent tip, which typically causes the cutting edge to be offset from the center of the cannula. Naemura et al. [61] found that a Tuohy needle with larger tip offset causes a steeper slope after puncture (larger drop in axial force), in both silicone rubber at 2, 4, and 8 mm/s ($n = 10$) and porcine ligamentum flavum at 8 mm/s ($n = 2$).

Suzuki et al. [14] compare the effect of tip shape details on axial force for two types of multi-faceted bevel tips ('Lancet' and 'Backcut', 20 G). They associate the force fluctuations observed with specific geometrical traits of the tip, but their experimental equipment does not include a means to verify whether these associations are accurate (e.g. synchronized imaging). No significant influence of tip type on peak forces was found.

In short, a diamond tip trocar needle was found to cause two distinct force peaks when inserted into porcine liver: a small one during puncture, and a large one during the transition from tip to shaft. Similar observations were made for beveled needles penetrating polyurethane and neoprene membranes at low speeds. A larger tip offset in Tuohy needles was found to cause a larger drop in force after puncture.

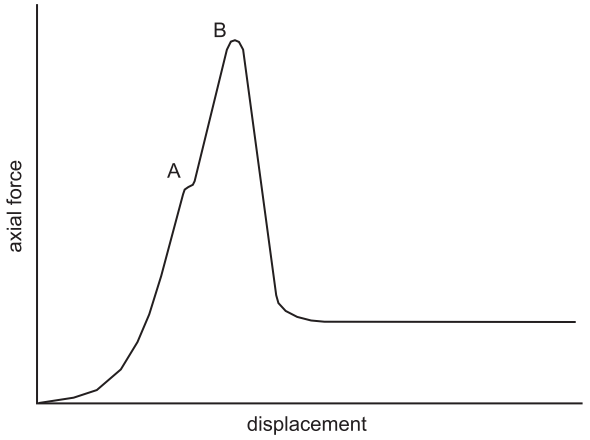

Fig. 13. Typical (idealized) axial force response during low speed membrane puncture with a beveled needle (similar to e.g. [24,13]). Point A indicates initial puncture, point B arises during the transition from bevel to shaft.

4.2.3. Bevel angle

Westbrook et al. [15] compared 26 G Quincke needles (multi-faceted bevel) from two different manufacturers during manual insertion into bovine dura ex vivo. They found a significantly higher puncture force for larger bevel angles (mean/std: 0.15/0.03 kgf vs. 0.03/0.01 kgf for $n = 10$). The bevel angles were not specified.

Okamura et al. [9] and O'Leary et al. [64] attempted to correlate axial forces and bevel angle for 1.0*mm* diameter beveled needles, with bevel angles of 10°, 14°, and 20°, inserted into silicone rubber at 2.65 mm/s. No significant effect was found.

Azar and Hayward [37] found indications (based on small samples) that crack length in porcine liver is approximately equal to needle diameter for a 22° bevel, but larger than diameter for 45° bevel.

Misra et al. [96] inserted large needle models of 15 mm diameter with bevel angles of 10–60° into three different Plastisol gels. The transverse force was found to decrease quickly with increasing bevel angle, starting at 4 N for 10° bevel angle and approaching zero at 45°.

Kataoka et al. [89] and Naemura [60] also considered the effect of tip angles, but methods and results are not clear.

In short, there are some indications that increased bevel angle may lead to higher axial forces and greater crack length.

4.2.4. Influence of the stylet

Most needles are equipped with a stylet that fits inside the lumen and prevents the accumulation of tissue during insertion. This stylet is usually flush with the tip, but so-called trocar needles have a cutting stylet which protrudes from the cannula.

It is not unthinkable that the presence of a stylet could influence the cutting behavior of the needle, since it influences the size of the contact area between needle tip and tissue. However, the presence of a stylet is not explicitly considered in any of the publications discussed here (except for the diamond tip trocar needles).

4.3. Sharpness

A sharp needle cuts more easily than a blunt one. The question is whether this effect is large enough to be of importance.

Westbrook et al. [15], Frick et al. [5], and Langevin et al. [51] used a new needle for each insertion. Nguyen et al. [63] re-used their needles up to five times, and Lewis et al. [54] used each of their needles for eight insertions into human dura. The latter used needles that had already been 'appropriately blunted' during actual epidural procedures.

Stellman [13] presents the only systematic investigation of sharpness. This was done by performing three subsequent penetrations of polyurethane membrane with each needle, using 22 G and 26 G beveled needles from different manufacturers, in combination with various lubricants. Successive insertions showed a statistically significant (although quite small) increase in peak force compared to the first insertion for the 26 G needle, irrespective of lubricant type. For the 22 G needle no significant influence was found.

In short, for 26 G beveled needles penetrating polyurethane membrane a small increase in axial force was observed in successive insertions.

4.4. Lubrication

Needles are typically covered with lubricant by the manufacturer.

Stellman [13] investigated the influence of different needle lubricants on peak insertion forces for (beveled) hypodermic needles, of different diameters (18 G, 22 G, 26 G, 30 G) and brands, inserted through a thin polyurethane membrane at 100 mm/min (1.7 mm/s). For all diameters a large (and significant) difference was found between peak forces for the lubricated needle and those for the bare needle (irrespective of lubricant type and needle manufacturer). The bare needles generated peak forces over two times as large as those for the lubricated needles. Variability was shown to be relatively small for sample sizes of 10 to 30 insertions per needle, and was smaller for lubricated needles than for bare needles.

Naemura et al. [61] found that the first insertion of their custom-made 18 G Tuohy needles into 3 mm thick silicone rubber membranes required consistently higher total axial force (in the order of 10%) than subsequent insertions (at new locations). Microscopic investigation of the needle surface after insertion showed traces of silicone, which may act as a lubricant.

In short, lubricant, irrespective of type, appears to have a large effect on peak axial force for beveled needles puncturing polyurethane membranes. However, it is not known whether this effect is also present in biological tissue. The fact that moisture is released due to cutting of biological tissue might play a role here. The influence of tissue properties is discussed next.

5. Influence of tissue characteristics

Of the 99 papers included in this survey, 38 considered artificial tissue in the form of porcine gelatin, PVC, Plastisol, silicone or similar materials.

In vitro measurements were performed on porcine tissue (25 papers), bovine tissue (12 papers), canine tissue (2), rabbit (1), chicken (4), turkey (3), sheep (2), and human (8) tissue, in a variety of organs, muscle being the most popular.

In vivo measurements were performed on human test subjects (14 papers), porcine subjects (8) and rabbits (5), again in a variety of organs, where skin (with underlying tissue) is most popular.

A table relating specific articles to combinations of organism, tissue type, and tissue condition is provided online as supplementary material.

The first question to be asked here is whether artificial tissue is a reliable substitute for biological tissue.

5.1. Artificial vs. biological

Artificial tissue offers many practical advantages over biological tissue, in terms of reproducibility, availability, visibility, etc. However, based on differences in microscopic structure between the two, most likely there will also be differences in needle–tissue interaction. For example, rubber or silicone phantoms may exhibit excessive frictional force. Whether the practical advantages of using artificial material outweigh the supposed lack of realism depends on the application.

The differences between artificial and biological tissue have not been investigated rigorously in any of the papers included in this survey. Nevertheless, the subject is touched upon in [57,58,61,62,9,64,67,16,71].

Meltsner et al. [57] inserted rotating and non-rotating conical needles into bovine muscle tissue and into a porcine gelatine phantom, at three different velocities. The axial force vs. position relation for the artificial phantom was approximately linear, contrary to that for the bovine muscle tissue, which was highly non-linear. The effect of insertion velocity is clearly distinguishable in the artificial phantom, whereas no such effect is seen in the muscle tissue. The influence of rotation on axial force is clearly visible in both artificial phantom and muscle tissue.

Misra et al. [58] determined the (effective) modulus of elasticity and the rupture toughness for Plastisol gel, porcine gel, and chicken breast. Although the mean modulus of elasticity was found to be comparable for all materials, mean rupture toughness for porcine gel was almost five times as high as for chicken breast. For Plastisol it was approximately twice as high as for chicken breast.

Reed et al. [67] investigated rotational friction acting on the shaft of a 24 G needle during rotational and translational motion, in various materials, by measuring the lag in rotation angle at the tip. Plastisol gel, porcine gel, ballistics gel, and chicken breast were investigated. Tip lag in chicken at a depth of 10 cm was found to be negligibly small (in the order of 1°), followed closely by soft Plastisol and hard Plastisol (in the order of 10°). In porcine gel the tip lag was approximately 30° and in ballistic gel it was as high as 45°. Porcine gel was found to exhibit the worst stick-slip behavior.

Shergold and Fleck [71] investigated insertion force and crack shape for beveled, conical, and blunt needles, inserted into two types of silicone rubber as well as into human skin in vivo and porcine skin in vitro. Inspection of microscopic images of the crack at the surface level indicated that crack shape depends on tip shape for both rubber and skin. This is the only paper found that attempts to justify the use of artificial phantoms using data from literature.

Naemura et al. [61,62] compared axial forces for Tuohy needles inserted into silicone rubber membranes and porcine ligamentum flavum. Peak axial force for the silicone rubber was found to be approximately three times as high as for the ligamentum flavum. Forces in an artificial phantom composed of melamine foam and latex rubber were found to be qualitatively and quantitatively similar to those in porcine ligaments.

In short, force-position curves in porcine gelatine were found to be linear, whereas in bovine tissue they were highly nonlinear. Axial force in gelatine was influenced both by velocity and rotation, but in bovine muscle it was only influenced by rotation. Although modulus of elasticity was comparable for chicken breast and several artificial materials, the rupture toughness of chicken breast was several times smaller. Indications were also found that friction in artificial materials is much higher than for chicken breast. Crack shapes were found to be similar in skin and silicone rubber.

5.2. Human tissue vs. other biological tissue

It would be useful to know to what extent animal tissue can be used as a substitute for human tissue, since the former can be obtained in greater quantities and is typically easier to work with. The difference between human tissue and tissue from other animals is discussed in [76,77,25,45], but an extensive systematic investigation of the influence on needle–tissue interaction forces was not found.

Brett et al. [76,77] investigated the force patterns encountered during epidural needle insertion (through skin and relevant ligaments). This was done by inserting Tuohy needles (unknown size) into recently deceased porcine samples (constant velocity) and into recently deceased human cadavers (manual insertion). The force-position curves were found to be qualitatively similar, but peak forces and friction forces in porcine tissue were much higher.

Hiemenz Holton [45] investigated insertion of 18 G Tuohy needles into human skin and fat (0.2 mm/s) and into porcine skin (0.1 mm/s). Mean peak axial force for porcine skin, as well as variability (although unspecified), were found to be over twice as high as those for human skin.

Okuno et al. [25] inserted 27 G and 21 G hypodermic needles through the skin into rabbit veins and human veins, both in vivo. The rabbit insertions ($n = 24$) were automated, whereas the human insertions ($n = 10$) were performed manually. It is concluded that the force patterns (in time) are qualitatively similar.

In short, penetration of porcine skin using Tuohy needles was found to require higher force than penetration of human skin. In vivo penetration of blood vessel, through the skin, delivered qualitatively similar force–time relations for both human and rabbit.

5.3. Live vs. dead biological tissue

In vivo measurements are typically more difficult to perform than ex vivo measurements, for practical as well as ethical reasons. Therefore it is very important to know if, and under which circumstances, ex vivo measurements can be used as a reliable substitute for in vivo measurements when investigating needle–tissue interaction.

No studies were found that systematically investigate the difference between living and dead tissue in terms of needle–tissue interaction. The subject is, however, touched upon in [44,90,84].

Heverly and Dupont [44] measured axial force during needle insertions into the hearts of very recently (10 min) deceased rabbits. They also performed ultrasound (US) guided needle insertions into rabbit hearts in vivo, without measuring force. It is concluded that puncture force is reduced at higher velocity both in vitro and in vivo.

Kobayashi et al. [90] inserted a 17 G beveled needle into porcine liver, both in vitro and in vivo. Data were used to identify the parameters of a non-linear finite element model. In vivo, the stiffness parameters were two to six times as high as in vitro.

Elagha et al. [84] punctured porcine interatrial septum (internal heart wall), both in vitro and in vivo, but no conclusions are drawn with respect to the difference between living or dead tissue.

In short, there are indications that velocity effects are present in rabbit heart tissue, both dead and alive. Live porcine liver was associated with higher stiffness values in a FE model.

5.4. Decay time

Only Choy et al. [40] explicitly investigate the influence of decay time on instrument–tissue interaction force. Strictly speaking, they use a RF-ablation catheter tip instead of a needle. A 12 G catheter was moved into porcine heart tissue (endocardium) in thee different areas, from 0.5 mm up to 4 mm penetration depth. This was done 15 min, 40 min, 3 h, 8 h and 18 h after death. The force at a given depth was found to increase with decay time. For example, at 4 mm depth, the force after 3 h was already twice as high as after 15 min, and after 18 h it was eight times as high. It is concluded that tissue properties can already change considerably within minutes after death.

Other authors also recognized the necessity to minimize (or mention) decay time. The following decay times were achieved with various tissues: 10 min human prostate [27,16]; 10*min* rabbit heart [44]; 2 h porcine liver [20]; 2 h bovine dura [15]; 2–5 h porcine back [76]; 3–6 h bovine liver [9]; 24 h canine back [87]; 24 h porcine liver [37]; 24–48 h porcine back [29]; and 26*h* porcine back [45].

Table 3
Main findings from C2 to C3 articles (for puncture, cutting, friction, and total force).

		F_p	F_c	F_f	F_{tot}
Velocity	Art			+	
	Bio	0/–		+	
Diameter	Art	+		+	
	Bio				+
Bevel angle	Art				0
	Bio	+			
# Tip edges	Art			–	
	Bio	–			+
Tip details	Art	+			
	Bio	+			0
Sharpness	Art				–
Lubricant	Art				–
Patient crit.	Bio				0
Location	Bio	0	0		
Art vs. bio					0

+, pos. correlation; –, neg. correlation; 0, no corr. or inconclusive.

5.5. Freezing and tissue hydration

The influence of freezing and thawing tissue, despite its potential to inflict damage on the tissue at a microscopic scale, is not investigated in any of the studies included in this survey. The effects of temperature, tissue hydration or perfusion, or rigor mortis are also neglected. Several authors do mention storing tissue in saline to prevent moisture loss [76,40,44,20,54,15,30,39].

Literature related to the food industry, e.g. Lawrie and Ledward [106] and Warriss [107], contains a wealth of information concerning the changes that take place in muscle tissue post-mortem. The influence of rigor mortis, moisture loss, and freezing are investigated there in relation to the tenderness of meat (after cooking).

6. Discussion

In the preceding sections, information regarding the influence of different variables on the axial force during needle insertion was presented, irrespective of classification.

However, in order to properly interpret the experimental data presented, information concerning sample size and variability is indispensable. Therefore only papers in the C2 and C3 classes are discussed here. The most important findings from these papers are summarized in Table 3, and a table with findings from all articles is available online as supplementary material.

6.1. Axial force characteristics

It is safe to say that the moment at which puncture (crack initiation) occurs depends on the stress levels in the tissue surrounding the needle tip, as described by Kobayashi et al. [7]. Moreover, in order to understand the puncture phenomenon, it is essential that

tissue displacements are measured in addition to needle displacement, as done by Kobayashi et al. [21].

As far as composition of the axial force is concerned, the (practically) linear increase in force with needle position, as observed by Hing et al. [19,20] in porcine liver, is consistent with the assumption that axial force is composed of a constant cutting force at the tip and a friction force that is uniformly distributed along the needle. The latter is also supported by the findings of Crouch et al. [17], for silicone gel.

6.2. Insertion method

It is clear that the mean *puncture force* in porcine heart decreases with increasing velocities up to 75 mm/s, after which it remains more or less constant, as shown by Mahvash and Dupont [8]. The variability of the puncture force in porcine liver was also found to decrease with increasing velocity, according to Kobayashi et al. [7] and Hing et al. [19,20].

On the other hand, velocity could not be shown to influence *cutting force* in porcine liver by Hing et al. [20], nor could a sound investigation by Frick et al. [5] uncover any influence of velocity on *peak axial force* when penetrating sheep skin.

It is likely that *friction force* in silicone gel is increased by increasing velocity, based on the increase in slope of the force-position curves found by Crouch et al. [17].

The investigation into the effect of insertion location in the human prostate by Podder et al. [27] and Yan et al. [16] came up inconclusive in this respect.

6.3. Needle characteristics

Quite some data, based on manual insertions in over fifty live human patients, is presented by Podder et al. [11,26,12] in support of the assumption that *peak axial force* is increased when needle diameter is increased. A similar conclusion was reached by Okuno et al. [25].

The type of needle also seems to be of influence: Conical needles were associated with a higher *peak axial force* than beveled needles when penetrating bovine dura, and large bevel angles required more force than small bevel angles [15]. Furthermore, *peak axial force* for diamond tip trocar needles was consistently higher than for beveled needles during insertion into porcine heart, despite the fact that the beveled needles had larger diameter [8].

The latter should be considered in light of the findings presented by Hing et al. [19,20], who observed that diamond tip trocar needles in porcine liver produce a small peak during puncture, followed by a much larger peak due to the transition from tip to shaft. A similar effect was found for beveled needles penetrating polyurethane film, e.g. by Stellman [13].

A decrease in slope of the force-position curve suggests that *friction force* in silicone rubber decreases with increasing number of cutting edges (conical → beveled → diamond) as found by Okamura et al. [9]. This effect was amplified by increased needle diameter.

Bevel shape details were not found to have a relevant effect on axial force by Suzuki et al. [14], nor was bevel angle [9].

6.4. Tissue characteristics

Forces during hypodermic needle insertion into human skin and into rabbit ears (both in vivo) were found to be qualitatively similar by Okuno et al. [25]. However, the actual influence of tissue characteristics on axial force during needle insertion remains a mystery.

7. Conclusion

A survey was presented of experimental needle–tissue interaction force data available in literature. This survey is organized in such a way that the reader can quickly find literature (useful for) investigating the influence of specific variables on axial force during needle insertion.

Although many studies did present force data, dedicated experimental investigations of the topics of interest were scarce and thinly spread. Therefore it was not possible to synthesize conclusive results from literature in the manner of a meta-analysis.

Nevertheless, good indications were found that puncture force decreases and friction force increases with increasing insertion velocity, and that needles with larger diameter typically cause higher peak forces, although the strength of these effects depends on the type of tissue. The highest force peaks during membrane puncture appear not to occur during initial penetration but slightly later, when the membrane is transferred from the tip to the shaft.

Many questions remain open for investigation, especially those related to biological tissue. For example, it is not clear whether artificial phantom materials provide a good alternative for biological tissue when investigating the effect of insertion velocity on axial force. Although the trends found for the influence of velocity on friction force were similar in both types of tissue, there were considerable quantitative differences.

Moreover, measuring forces in vivo is substantially more difficult, both in a practical sense and in an ethical sense, than measuring forces ex vivo. Therefore it would be interesting to know to what extent ex vivo measurements can be used as a substitute for in vivo measurements. The same goes for using animal tissue as a substitute for human tissue. However, this survey was not able to shed sufficient light on these issues.

Seeing that variability is typically high when dealing with biological tissue, it is difficult to interpret experimental data without some indication of both the variability and the sample size. Out of 99 papers, 73 did not report these values.

Appendix A. Supplementary data

Supplementary data associated with this article can be found, in the online version, at http://dx.doi.org/10.1016/j.medengphy.2012.04.007.

Conflict of interest statement

No conflict of interest to report.

References

[1] Abolhassani N, Patel R, Moallem M. Needle insertion into soft tissue: a survey. Med Eng Phys 2007;29:413–31.
[2] Misra S, Ramesh KT, Okamura AM. Modeling of tool-tissue interactions for computer-based surgical simulation – a literature review. Presence-Teleop Virt Environ 2008;17(5):463–91.
[3] Cowan NJ, Goldberg K, Chirikjian GS, Fichtinger G, Alterovitz R, Reed KB, et al. Robotic needle steering: design, modeling, planning, and image guidance. In: Rosen J, Hannaford B, Satava RM, editors. Surgical Robotics: Systems Applications and Visions, vol. 3. Springer; 2011. p. 557–82.
[4] Trejos A, Patel R, Naish M. Force sensing and its application in minimally invasive surgery and therapy: a survey. P I Mech Eng C-J Mech 2010;224:1435–54.
[5] Frick T, Marucci D, Cartmill J, Martin C, Walsh W. Resistance forces acting on suture needles. J Biomech 2001;34:1335–40.
[6] Jensen W, Yoshida K, Hofmann UG. In vivo implant mechanics of single-shaft microelectrodes in peripheral nervous tissue. In: IEEE EMBS conference on neural engineering. 2007. p. 1–4.
[7] Kobayashi Y, Onishi A, Hoshi T, Kawamura K. Modeling of conditions where a puncture occurs during needle insertion considering probability distribution. In: IEEE/RSJ international conference on intelligent robots and systems. 2008. p. 1433–40.
[8] Mahvash M, Dupont PE. Mechanics of dynamic needle insertion into a biological material. IEEE Trans Biomed Eng 2010;57(4):934–43.

[9] Okamura AM, Simone C, O'Leary MD. Force modeling for needle insertion into soft tissue. IEEE Trans Biomed Eng 2004;51(10):1707–16.
[10] Passerotti CC, Begg N, Penna FJ, Passerotti AMA, Leite KR, Antunes AA, et al. Safety profile of trocar and insufflation needle access systems in laparoscopic surgery. J Am Coll Surg 2009;209(2):222–32.
[11] Podder T, Clark D, Sherman J, Fuller D, Messing E, Rubens D, et al. In vivo motion and force measurement of surgical needle intervention during prostate brachytherapy. Med Phys 2006;33(8):2915–22.
[12] Podder TK, Sherman J, Messing EM, Rubens DJ, Fuller D, Strang JG, et al. Needle insertion force estimation model using procedure-specific and patient-specific criteria. In: 28th Annual international conference of the IEEE EMBS. 2006. p. 555–8.
[13] Stellman JT. Development, production, and characterization of plastic hypodermic needles. Master's thesis. Georgia Institute of Technology; 2009.
[14] Suzuki T, Tanaka A, Fukuyama H, Nishiyama J, Kanazawa M, Oda M, et al. Differences in penetration force of intravenous catheters – effect of grinding methods on inner needles of intravenous catheters. Tokai J Exp Clin Med 2004;29(4):175–81.
[15] Westbrook JL, Uncles DR, Sitzman BT, Carrie LES. Comparison of the force required for dural puncture with different spinal needles and subsequent leakage of cerebrospinal fluid. Anesth Analg 1994;79:769–72.
[16] Yan K, Podder T, Li L, Joseph J, Rubens DR, Messing EM, et al. A real-time prostate cancer detection technique using needle insertion force and patient-specific criteria during percutaneous intervention. Med Phys 2009;36(7):3356–62.
[17] Crouch JR, Schneider CM, Wainer J, Okamura AM. A velocity-dependent model for needle insertion in soft tissue. In: Lecture notes in computer science. Berlin: Springer Berlin/Heidelberg; 2005. p. 624–32.
[18] Gossot D, Validire P, Matsumoto S, Tokumura H, Shimomura K, Flowers J, et al. Development of an ultrasonically activated trocar system. Surg Endosc 2002;16:210–4.
[19] Hing JT, Brooks AD, Desai JP. Reality-based needle insertion simulation for haptic feedback in prostate brachytherapy. In: IEEE international conference on robotics and automation, ICRA 2006. 2006. p. 619–24.
[20] Hing JT, Brooks AD, Desai JP. A biplanar fluoroscopic approach for the measurement, modeling, and simulation of needle and soft-tissue interaction. Med Image Anal 2007;11:62–78.
[21] Kobayashi Y, Sato T, Fujie MG. Modeling of friction force based on relative velocity between liver tissue and needle for needle insertion simulation. In: 31st Annual international conference of the IEEE EMBS. 2009. p. 5274–8.
[22] Matsumiya K, Momoi Y, Kobayashi E, Sugano N, Yonenobu K, Inada H, et al. Analysis of forces during robotic needle insertion to human vertebra. In: Lecture notes in computer science, vol. 2878. Berlin: Springer; 2003. p. 271–8.
[23] Mayer G, Knappertz V, Kinast P, Needles: a comparison study. Tech. Rep., European Medical Device Technology; 2009.
[24] Mueller F. Biomechanical test report on hsw fine-ject needles. Tech. Rep.; Henke-Sass Wolf GmbH; 2011.
[25] Okuno D, Togawa T, Saito H, Tsuchiya K. Development of an automatic blood sampling system: control of the puncturing needle by measuring forces. In: 20th Annu. Int. Conf. of the IEEE Eng. in medicine and biology soc. 1998. p. 1811–2.
[26] Podder TK, Sherman J, Fuller D, Messing EM, Rubens DJ, Strang JG, et al. In-vivo measurement of surgical needle intervention parameters: a pilot study. In: 28th Annual international conference of the IEEE EMBS. 2006. p. 3652–5.
[27] Podder TK, Sherman J, Li L, Joseph J, Rubens DR, Messing EM, et al. Mechanical properties of human prostate tissue in the context of surgical needle insertion. Int J Comp Assist Radiol Surg 2007;2:S82–133.
[28] Saito H, Togawa T. Detection of needle puncture to blood vessel using puncture force measurement. Med Biol Eng Comput 2005;43:240–4.
[29] Tran D, Hor Kw, Kamani AA, Lessoway VA, Rohling RN. Instrumentation of the loss-of-resistance technique for epidural needle insertion. IEEE Trans Biomed Eng 2009;56(3):820–7.
[30] Wittek A, Dutta-Roy T, Taylor Z, Horton A, Washio T, Chinzei K, et al. Subject-specific non-linear biomechanical model of needle insertion into brain. Comput Meth Biomech Biomed Eng 2008;11(2):135–46.
[31] Abolhassani N, Patel R, Moallem M. Experimental study of robotic needle insertion in soft tissue. Int Congr Ser 2004;1268:797–802.
[32] Abolhassani N, Patel R, Moallem M. Trajectory generation for robotic needle insertion in soft tissue. In: 26th Annual international conference of the IEEE EMBS. 2004. p. 2730–3.
[33] Abolhassani N, Patel R, Moallem M. Control of soft tissue deformation during robotic needle insertion. Minim Invasiv Ther 2006;15(3):165–76.
[34] Abolhassani N, Patel R, Ayazi F. Minimization of needle deflection in robot-assisted percutaneous therapy. Int J Med Robot Comp 2007;3:140–8.
[35] Asadian A, Kermani MR, Patel RV. A compact dynamic force model for needle–tissue interaction. In: 32nd Annual international conference of the IEEE EMBS. 2010. p. 2292–5.
[36] Asadian A, Patel RV, Kermani MR. A distributed model for needle–tissue friction in percutaneous interventions. In: IEEE International conference on robotics and automation. Shanghai, China: IEEE; 2011. p. 1896–901.
[37] Azar T, Hayward V. Estimation of the fracture toughness of soft tissue from needle insertion. In: Bello F, Edwards E, editors. Lecture Notes in Computer Science, vol. 5104. Berlin: Springer-Verlag; 2008. p. 166–75.
[38] Badaan S, Petrisor D, Kim C, Mozer P, Mazilu D, Gruionu L, et al. Does needle rotation improve lesion targeting. Int J Med Robotics Comput Assist Surg 2011;7:138–47.
[39] Bzostek A, Kumar R, Diaz L, Svrivastava M, Anderson JH, Taylor RH. Force vs deformation in soft tissue puncture. MICCAI 1999, http://dx.doi.org/10.1.1.37.6345.
[40] Choy YB, Cao H, Tungjitkusolmun S, Tsai JZ, Haemmerich D, Vorperian VR, et al. Mechanical compliance of the endocardium. J Biomech 2002;35:1671–6.
[41] DiMaio SP, Salcudean SE. Needle insertion modelling and simulation. In: IEEE international conference on robotics and automation, ICRA 2002. 2002. p. 2098–105.
[42] DiMaio SP, Salcudean SE. Needle insertion modeling and simulation. IEEE Trans Robotic Autom 2003;19(5):864–75.
[43] Healey AE, Evans JC, Murphy MG, Powell S, How TV, Groves D, et al. In vivo force during arterial interventional radiology needle puncture procedures. In: Westwood J, editor. St Heal T, vol. 13. IOS Press; 2005, p. 178–84.
[44] Heverly M, Dupont P. Trajectory optimization for dynamic needle insertion. In: IEEE international conference on robotics and automation, ICRA 2005. Barcelona, Spain; 2005. p. 1658–63.
[45] Hiemenz Holton LL. Force models for needle insertion created from measured needle puncture data. In: Westwood J, editor. St heal T. IOS Press; 2001. p. 180–6.
[46] Howard MA, Abkes BA, Ollendieck MC, Noh MD, Ritter RC, Gillies GT. Measurement of the force required to move a neurosurgical probe through in vivo human brain tissue. IEEE Trans Biomed Eng 1999;46(7):891–4.
[47] Kataoka H, Washio T, Chinzei K, Mizuhara K, Simone C, Okamura AM. Measurement of the tip and friction force acting on a needle during penetration. In: Lecture notes in computer science, vol. 2488. Berlin: Springer Berlin /Heidelberg; 2002. p. 216–23.
[48] Kobayashi Y, Onishi A, Watanabe H, Hoshi T, Kawamura K, Hashizume M, et al. Development of an integrated needle insertion system with image guidance and deformation simulation. Comput Med Imag Grap 2010;34:9–18.
[49] Kong X, Wu C. Measurement and prediction of insertion force for the mosquito fascicle penetrating into human skin. J Bionic Eng 2009;6(2):143–52.
[50] Lagerburg V, Moerland MA, Konings MK, van de Vosse RE, WLagendijk JJ, Battermann JJ. Development of a tapping device: a new needle insertion method for prostate brachytherapy. Phys Med Biol 2006;51:891–902.
[51] Langevin HM, Churchill DL, Fox JR, Badger GJ, Garra BS, Krag MH. Biomechanical response to acupuncture needling in humans. J Appl Physiol 2001;91:2471–8.
[52] Lechner TJ, van Wijk MG, Maas AJ, van Dorsten FR, Drost RA. Langenberg C.J., et al. Clinical results with the acoustic puncture assist device, a new acoustic device to identify the epidural space. Anesth Analg 2003;96:1183–7.
[53] Lechner T, van Wijk M, Maas A, van Dorsten F. Thoracic epidural puncture guided by an acoustic signal: clinical results. Eur J Anaesth 2004;21:694–9.
[54] Lewis MC, Lafferty JP, Sacks MS, Pallares VS, TerRiet M. How much work is required to puncture dura with tuohy needles? Brit J Anaesth 2000;85(2):238–41.
[55] Mahvash M, Dupont PE. Fast needle insertion to minimize tissue deformation and damage. In: IEEE international conference on robotics and automation, ICRA 2009. 2009. p. 3097–102.
[56] Maurin B, Barbe L, Bayle B, Zanne P, Gangloff J, De Mathelin M, et al. In vivo study of forces during needle insertions. In: Medical robotics, navigation and visualisation scientific workshop. 2004. p. 415–22.
[57] Meltsner M, Ferrier N, Thomadsen B. Observations on rotating needle insertions using a brachytherapy robot. Phys Med Biol 2007;52:6027–37.
[58] Misra S, Reed KB, Douglas AS, Ramesh KT, Okamura AM. Needle–tissue interaction forces for bevel-tip steerable needles. In: IEEE/RAS-EMBS international conference on biomedical robotics and biomechatronics. 2008. p. 224–31.
[59] Misra S, Reed K, Schafer B, Ramesh K, Okamura A. Mechanics of flexible needles robotically steered through soft tissue. Int J Robot Res 2010;29(13):1640–60.
[60] Naemura K. Comparative phantom study on epidural anesthesia needle. In: 28th Annual international conference of the IEEE EMBS. 2006. p. 4995–8.
[61] Naemura K, Uchino Y, Saito H. Effect of the needle tip height on the puncture force in a simplified epidural anesthesia simulator. In: 29th Annual international conference of the IEEE EMBS. 2007. p. 3504–7.
[62] Naemura K, Sakai A, Hayashi T, Saito H. Epidural insertion simulator of higher insertion resistance and drop rate after puncture. In: 30th Annual international conference of the IEEE EMBS. 2008. p. 3249–52.
[63] Nguyen CT, Vu-Khanh T, Dolez PI, Lara J. Puncture of elastomer membranes by medical needles. Part I: mechanisms. Int J Fract 2009;155:75–81.
[64] O'Leary MD, Simone C, Washio T, Yoshinaka K, Okamura AM. Robotic needle insertion: effects of friction and needle geometry. In: IEEE international conference on robotics and automation, ICRA 2003. 2003. p. 1774–80.
[65] Podder TK, Clark DP, Fuller D, Sherman J, Ng WS, Liao L, et al.IEEE Eng Med Biol. 2005. p. 5766–70.
[66] Podder TK, Sherman J, Clark DP, Messing EM, Rubens DJ, Strang JG, et al. Evaluation of robotic needle insertion in conjunction with in vivo manual insertion in the operating room. In: IEEE International workshop on robots and human interactive communication. 2005. p. 66–72.
[67] Reed KB, Okamura AM, Cowan NJ. Controlling a robotically steered needle in the presence of torsional friction. In: IEEE international conference on robotics and automation, ICRA 2009. 2009. p. 3476–81.

[68] Roy J, Roesthuis Youri RJ, van Veen AJ, Misra S. Mechanics of needle–tissue interaction. In: IEEE/RSJ international conference on intelligent robots and systems. San Francisco, CA, USA: IEEE; 2011. p. 2557–63.
[69] Saito H, Togawa T. Detection of puncturing blood vessel wall for automatic blood sampling. In: The first joint BMES/EMBS conference serving humanity, advancing technology. 1999. p. 866.
[70] Schneider C.M., Crouch J.R., Okamura A.M. Modeling and measuring the dynamic 3d effects of needle insertion in soft tissue. Tech. Rep. 04-1, The Johns Hopkins University, 2004.
[71] Shergold OA, Fleck NA. Experimental investigation into the deep penetration of soft solids by sharp and blunt punches, with application to the piercing of skin. J Biomech Eng 2005;127(5):838–48.
[72] Simone C. Modeling of needle insertion forces for percutaneous therapies. Master's thesis, The Johns Hopkins University; 2002.
[73] Simone C, Okamura AM. Modeling of needle insertion forces for robot-assisted percutaneous therapy. In: IEEE international conference on robotics and automation, ICRA 2002. 2002. p. 2085–91.
[74] Abolhassani N, Patel R. Deflection of a flexible needle during insertion into soft tissue. In: 28th Annual international conference of the IEEE EMBS. 2006. p. 3858–61.
[75] Barbe L, Bayle B, de Mathelin M, Gangi A. Online robust model estimation and haptic clues detection during in vivo needle insertions. In: IEEE international conference on biomedical robotics and biomechatronics. 2006. p. 341.
[76] Brett PN, Parker T, Harrison AJ, Thomas TA, Carr A. Simulation of resistance forces acting on surgical needles. P I Mech Eng H 1997;211:335–47.
[77] Brett PN, Harrison AJ, Thomas TA. Schemes for the identification of tissue types and boundaries at the tool point for surgical needles. IEEE Trans Inf Technol Biomed 2000;4(1):30–6.
[78] Brouwer I, Ustin J, Bentley L, Sherman A, Dhruv N, Tendick F. Measuring in vivo animal soft tissue properties for haptic modeling in surgical simulation. In: Westwood JDea, editor. St heal T. IOS Press; 2001. p. 69–74.
[79] Dehghan E, Wen X, Zahiri-Azar R, Marchal M, Salcudean SE. Modeling of needle–tissue interaction using ultrasound-based motion estimation. In: Lecture notes computer science; vol. 4791. Springer Berlin /Heidelberg; 2007. p. 709–16.
[80] Dehghan E, Wen X, Zahiri-Azar R, Marchal M, Salcudean SE. Parameter identification for a needle–tissue interaction model. In: 29th annual international conference of the IEEE EMBS. 2007. p. 190–3.
[81] Dehghan E, Salcudean SE. Needle insertion study using ultrasound-based 2d motion tracking. In: Metaxas D, editor. Lecture notes computer science; vol. 5242. Berlin: Springer-Verlag; 2008. p. 660–7.
[82] DiMaio SP, Salcudean SE. Simulated interactive needle insertion. In: 10th IEEE symposium On haptic interfaces for virtual environments and teleoperator systems. 2002. p. 344.
[83] DiMaio SP, Salcudean SE. Interactive simulation of needle insertion models. IEEE Trans Biomed Eng 2005;52(7):1167–79.
[84] Elagha AA, Kim AH, Kocaturk O, Lederman RJ. Blunt atrial transseptal puncture using excimer laser in swine. Catheter Cardio Inte 2007;70:585–90.
[85] Fazal I, Karsiti MD. Needle insertion forces for haptic feedback device. In: IEEE symposium on industrial electronics and applications. 2009. p. 20–2.
[86] Hiemenz L, Litsky A, Schmalbrock P. Puncture mechanics for the insertion of an epidural needle. In: 21st annual meeting of the American society of biomechanics. Clemson: SC; 1997.
[87] Hiemenz L, Stredney D, Schmalbrock P. Development of the force feedback model for an epidural needle insertion simulator. In: Westwood J, Hoffman H, editors. St heal T. IOS Press; 1998. p. 272–7.
[88] Hungr N, Troccaz J, Zemiti N, Tripodi N. Design of an ultrasound-guided robotic brachytherapy needle-insertion system. In: 31st Annual international conference of the IEEE EMBS. 2009. p. 250–3.
[89] Kataoka H, Noda S, Yokota H, Takagi S, Himeno R, Okazawa S. Simulations of needle insertion by using a eulerian hydrocode fem and the experimental validations. In: Lecture notes in computer science, vol. 5242. Berlin: Springer; 2008. p. 560–8.
[90] Kobayashi Y, Onishi A, Hoshi T, Kawamura K, Hashizume M, Fujie MG. Development and validation of a viscoelastic and nonlinear liver model for needle insertion. Int J Comp Assist Radiol Surg 2009;4(1):53–63.
[91] Kobayashi Y, Suzuki M, Konishi K, Hashizume M, Fujie MG. Development of a novel approach, palpation based needle insertion, for breast cancer treatment. In: IEEE international conference on robotics and biomimetics. 2009. p. 505–11.
[92] Kobayashi Y, Akinori O, Watanabe H, Hoshi T, Kawamura K, Fujie MG. Developing a planning method for straight needle insertion using probability-based condition where a puncture occurs. In: IEEE international conference on robotics and automation, ICRA 2009. 2009. p. 3482–9.
[93] Kobayashi Y, Suzuki M, Kato A, Konishi K, Hashizume M, Fujie MG. A robotic palpation-based needle insertion method for diagnostic biopsy and treatment of breast cancer. In: IEEE/RSJ international conference on intelligent robots and systems. 2009. p. 5534–9.
[94] Kokes R, Lister K, Gullapalli R, Zhang B, MacMillan A, Richard H, et al. Towards a teleoperated needle driver robot with haptic feedback for RFA of breast tumors under continuous MRI. Med Image Anal 2009;13:445–55.
[95] Lendvay TS, Hsieh FJ, Hannaford B, Rosen J. The Biomechanics of Percutaneous Needle Insertion. Newport Beach, CA: St Heal T; 2008.
[96] Misra S, Reed KB, Ramesh KT, Okamura AM. Observations of needle–tissue interactions. In: 31st Annual international conference of the IEEE EMBS. 2009. p. 262–5.
[97] Nguyen CT, Vu-Khanh T, Dolez PI, Lara J. Puncture of elastomer membranes by medical needles. part ii: Mechanics. Int J Fract 2009;155:83–91.
[98] Tse ZTH, Elhawary H, Rea M, Young I, Davis BL, Lamperth M. A haptic unit designed for magnetic-resonance-guided biopsy. P I Mech Eng H 2009;223:159–72.
[99] Vidal FP, John NW, Healey AE, Gould DA. Simulation of ultrasound guided needle puncture using patient specific data with 3d textures and volume haptics. Comput Anim Virtual Worlds 2008;19:111–27.
[100] Wiksell H, Ekstrand V, Wadstrom C, Auer G. A new semi-automated instrument to improve the fine needle aspiration procedure during breast lesion cell sampling. Phys Med 2009;25:128–32.
[101] Xie Y, Sun D, Liu C, Cheng SH, Liu YH. A force control based cell injection approach in a bio-robotics system. In: IEEE international conference on robotics and automation, ICRA 2009. 2009. p. 3443–8.
[102] Xu W, Frank TG, Cuschieri A. Development of a shape memory alloy multiple-point injector for chemotherapy. P I Mech Eng H 2005;219:213–7.
[103] Zivanovic A, Davies BL. A robotic system for blood sampling. IEEE Trans inf Technol Biomed 2000;4(1):8–14.
[104] Selvadurai A. Deflections of a rubber membrane. J Mech Phys Solids 2006;54:1093–119.
[105] Mahvash M, Hayward V. Haptic rendering of cutting: a fracture mechanics approach. Haptics-e 2001;2(3):1–12.
[106] Lawrie RA, Ledward DA. Lawrie's meat science. 2nd ed. Cambridge: Woodhead Publishing Limited; 2006.
[107] Warriss PD. Meat science: an introductory text. 2nd ed. Oxfordshire: CABI; 2010.